Available online at www.sciencedirect.com
SCIENCE DIRECT®
Polymer 44 (2003) 7441–7447
polymer
www.elsevier.com/locate/polymer

Preparation and membrane performance of poly(ethylene-*co*-vinyl alcohol) hollow fiber membrane via thermally induced phase separation

Mengxian Shang[a], Hideto Matsuyama[a,*], Masaaki Teramoto[a], Douglas R. Lloyd[b], Noboru Kubota[c]

[a]*Department of Chemistry and Materials Technology, Kyoto Institute of Technology, Matsugasaki, Sakyo-ku, Kyoto 606-8585, Japan*
[b]*Department of Chemical Engineering, The University of Texas at Austin, Austin, TX 78712, USA*
[c]*Asahi Chemical Industry Co., Ltd. 2-1 Samejima, Fuji, Shizuoka 416-8501, Japan*

Received 25 April 2003; received in revised form 22 July 2003; accepted 21 August 2003

Abstract

Poly(ethylene-*co*-vinyl alcohol) (EVOH) hollow fiber membranes with ultrafiltration performance were prepared from EVOH/glycerol systems via thermally induced phase separation (TIPS). The diluent glycerol was used as bore liquid to make a lumen of the hollow fiber for the purpose of prevention of the diluent evaporation and the larger pores formation at the inner surface of the hollow fiber. The obtained hollow fiber membranes showed asymmetric structures with skin layer near the outer surface, the larger pores just below the skin layer and the smaller pores near the inner surface. The formation of the larger pores near the outer surface was due to the enhanced pore growth by the water penetration. Some primary factors affecting the structure and performance of the membranes such as ethylene content (EC) in EVOH, cooling water bath temperature and take-up speed were studied extensively. The water permeability can be improved by increasing the water bath temperature and the take-up speed and by decreasing the EC. Both the pore size at the outer surface and the connectivity between the pores have to be considered together to understand the experimental result of the water permeability and the solute rejection.

Keywords: thermally induced phase separation; poly(ethylene-co-vinyl alcohol); hollow fiber membrane

1. Introduction

A great deal of attention has been paid to the possibility of utilizing the hollow fiber membranes for solute rejection in reverse osmosis (RO), ultrafiltration (UF) and microfiltration (MF), since the productivity and the efficiency of the separation process can be largely improved due to the large surface area per unit volume of the fiber module [1,2]. For the membrane preparation, the thermally induced phase separation (TIPS) method has been extensively used to form porous membranes, and the membrane structure was examined mainly from the basic standpoints of thermodynamics and kinetics [3–11]. However, the use of TIPS for the formation of hollow fiber membranes has not been widely reported.

Kim et al. [12] prepared polypropylene hollow fiber membranes from polypropylene/soybean oil mixture by the TIPS process and subsequent cold-stretching. Increased melt-draw ratio (defined as the ratio of take-up speed to the extrusion rate of the polymer solution) enhanced the formation of the micropores and fibril structure. The cold-stretching of the hollow fiber membranes remarkably increased the membrane porosity. Sun et al. [13] studied some major factors in high-density polyethylene (HDPE) hollow fibre membrane formation via TIPS process. The water permeability of HDPE hollow fiber membrane was sensitively influenced by the factors that govern the TIPS process of the HDPE/liquid-paraffin (LP) system. Water permeability of the membrane increased with increasing the LP content in the polymer solution and decreasing the membrane thickness. In our laboratory, HDPE hollow fiber membranes were also prepared via the TIPS process [14]. Two kinds of diluents such as diisodecyl phthalate (DIDP) and LP were used in the membrane preparation. The shorter air gap and the higher bath temperature were effective to obtain the higher water permeability. The liquid–liquid phase separation in the case of DIDP led to the higher

* Corresponding author. Tel.: +81-75-724-7542; fax: +81-75-724-7580.
E-mail address: matuyama@chem.kit.ac.jp (H. Matsuyama).

0032-3861/$ - see front matter © 2003 Elsevier Ltd. All rights reserved.
doi:10.1016/j.polymer.2003.08.033

permeability than the polymer crystallization in the case of LP.

In this study, poly(ethylene-*co*-vinyl alcohol) (EVOH) was used as a polymer for the hollow fiber membrane preparation via TIPS process, since EVOH copolymer with a hydrophilic segment, as asserted in a patent [15], has many superior properties over other hydrophobic polymers for the prevention of membrane fouling in the water treatment application. In our previous articles [16,17], the phase diagrams and structure growth mechanism were clarified in EVOH/glycerol systems. These thermodynamics and kinetics can be utilized to control the pore structure of the hollow fiber membrane. The objective of this work is to provide the fundamental knowledge necessary to prepare hollow fiber membranes by TIPS. The effects of several preparation conditions on water permeability and solute rejection were investigated in connection with the morphologies of the membranes.

2. Experimental

2.1. Materials

Three kinds of EVOHs with ethylene contents (EC) of 32, 38, and 44 mol% (abbreviated as EVOH32, EVOH38, and EVOH44, henceforth) were supplied from Nihon Gohsei Chemical Industry Co., Ltd, Japan. The properties of EVOHs are listed in Table 1. Glycerol (Wako Pure Chemical Industries, Ltd, Kyoto, Japan) was used as a diluent. All chemicals were used without further purification.

2.2. Determination of phase diagram

Cloud point (T_{cloud}) and crystallization temperature (T_c) were measured by the method similar to that previously used [16]. Homogeneous polymer-diluent samples were prepared by an IMC-119D mixer with a twin-blade (Imoto Co., Kyoto, Japan). Thirty grams of blended solutions were placed into the vessel, heated to 180 °C, and then mixed for 7 min at 50 rpm of rotating speed. The obtained homogeneous sample was placed between a pair of microscope cover slips. A 100 μm-thick Teflon film with a square opening was inserted between the cover slips. The sample was heated on an LK-600 PH hot stage (Linkam, Surrey, UK) to 200 °C for 1 minute and cooled to 25 °C at a controlled rate of 1 °C/min. Subsequently, T_{cloud} was determined visually by noting the appearance of turbidity under a BX50 optical microscope (Olympaus, Tokyo, Japan).

A Perkin–Elmer DSC-7 was used to determine the dynamic crystallization temperature. The sample was sealed in an aluminum differential scanning calorimetry (DSC) pan, melted at 200 °C for 3 min, and then cooled at a 10 °C/min to 50 °C. The onset of the exothermic peak during the cooling was taken as the crystallization temperature.

Table 1
Properties of EVOHs

	EVOH32	EVOH38	EVOH44
Ethylene content (mol%)	32	38	44
Density (g/cm^3)	1.19	1.17	1.14
Melting point (°C)	183	173	164
Crystallization temperature (°C)	160	152	144
MFR[a] (g/10 min)	3.2	3.2	3.5

Note: all of the data are provided by the manufacture.
[a] 210 °C, 21.168 N.

2.3. Light scattering measurements

The light scattering measurement was carried out to obtain structure growth data with a polymer dynamics analyzer (Otsuka Electronics Co., DYNA-1100T) [17]. The hot stage was located between a He–Ne laser (5 mW) and a detector. 25 wt% of EVOH44, EVOH38, and EVOH32 samples were sealed with two cover slips, placed on the stage, and then heated to 200, 160, and 160 °C, respectively. Then the sample was cooled to 40 °C at the rate of 130 °C/min. The structure growth behavior during the cooling was monitored at the time interval of 0.1 s by the light scattering measurement.

2.4. Hollow fiber membrane preparation

Hollow fiber membranes were prepared by a batch-type extruder (Imoto Co. BA-0, Kyoto, Japan) [14,18]. Measured amounts of EVOH and glycerol were fed to the vessel, heated to 200 °C for EVOH44 or 140 °C for EVOH38 and EVOH32 under the nitrogen atmosphere, and then mixed for 15 min. A short twin-screw was employed in the vessel to ensure the complete mixing by scraping the wall of the vessel. The polymer concentration was fixed at 25 wt%. After holding at this high temperature for 1 hour, the homogeneous polymer solution was fed to a spinneret by a gear pump under the nitrogen pressure of 0.15 MPa. The spinneret consists of outer and inner tubes, and their diameters were designed to be 1.58 mm and 0.83 mm, respectively. In contrast to the studies described above [12,13], the diluent was used instead of nitrogen to be introduced into the inner orifice to make a lumen of the hollow fiber for the purpose of the prevention of the diluent evaporation and the larger pores formation at the inner surface of the hollow fiber. The hollow fiber was extruded from the spinneret and wound on a take-up winder after entering into a water bath kept at a certain temperature to induce the phase separation and solidify the membrane. The diluent remaining in the hollow fiber product was extracted by immersing them into water. The variables in the spinning process were the water bath temperature and the take-up speed. The preparation conditions of each hollow fiber

membrane are listed in Table 2. The air gap distance, which is the distance from the spinneret to the water bath was 5 mm in all experiments. The extrusion rate of polymer solution and the bore liquid flow rate were fixed at about 0.1 and 0.27 m/s, respectively.

2.5. Characterization of the hollow fiber membrane

To obtain the dry membrane, the prepared membranes were immersed in water to extract the remaining diluent, and freeze-dried with an FD-1000 freeze dryer (Tokyo RIKAKIKAI Co., Tokyo, Japan). The dry hollow fiber membrane was fractured in liquid nitrogen and treated with Au/Pd sputtering. The cross sections and the surfaces of the hollow fiber membranes were examined using an S-800 scanning electron microscope (Hitachi Co., Tokyo, Japan) with an accelerating voltage of 20 kV.

Water permeability through the hollow fiber membrane was measured by a method similar to that described by Saito et al. [19]. Pure water was forced to permeate from the inside to the outside of the hollow fiber membrane. The transmembrane pressure could be applied by adjusting the pressure valve close to the release side, and the average of the readings of the two pressure gauges was taken as the feed pressure. The water permeability was calculated on the basis of the inner surface area of the hollow fiber membrane.

The filtration experiment was performed using the same apparatus as that used in the water permeation test. The solutes used were mono-dispersed polystyrene latex particles with various diameters of 100, 50 and 20 nm (Duke Scientific Co., Palo Alto, CA). The feed solutions were prepared by dispersing the latex particles in an aqueous non-ionic surfactant solution (0.1 wt% Triton X-100). The solute concentrations in the filtrate and feed solution were measured with an U-200 UV spectrophotometer (Hitachi Co., Tokyo, Japan) under the wavelength of 385 nm.

3. Results and discussion

3.1. Phase diagram

The phase diagrams of various EVOHs systems are shown in Fig. 1. The binodal line shifted to the higher temperature region as the EC in EVOH increased. For EVOH44, three binodal points were observed at the polymer concentrations less than 40 wt%. For EVOH38, only one binodal point was detected at the polymer concentration of 20 wt% sample, while no binodal point was observed in the polymer concentration region higher than 20 wt% for EVOH32. This is because the compatibility between EVOH and glycerol becomes better when the EC decreases [16] and thus, the cloud point of EVOH32 shifted below the crystallization temperature.

3.2. Kinetic study

The phase separation kinetics was studied by the light scattering measurement for EVOH44, EVOH38 and EVOH32 systems. In order to make the experimental condition of light scattering closer to the quench condition of hollow fiber membrane preparation, the cooling rate was kept at 130 °C/min, which was the maximum cooling rate of the hot stage. The light scattering result obtained in EVOH38 system is shown in Fig. 2. The similar patterns of light scattering curves in other two systems were also obtained even though they are not shown here. In all systems, the scattered light intensity I_s showed maximum in the plot of I_s against the scattered angle, and the position of the maximum of intensity was shifted to the lower scattered angle region with the elapse of time. This means that the phase separation occurred by the spinodal decomposition (SD) and the structure formed by the phase separation became larger with time [20]. The interphase periodic distance Λ can be related to the scattered angle θ where I_s

Table 2
Preparation conditions of EVOH hollow fiber membranes

Preparation conditions		EVOH32	EVOH38		EVOH44
1. Polymer concentration (wt%)		25	25		25
2. Mixing temperature (°C)		140	140		200
3. Rotation speed for mixing (rpm)		100	100		100
4. Extruding temperature (°C)		160	140		180
5. Mixing time (min)		15	15		15
6. Holding time at mixing temperature (min)		60	60		60
7. Air gap (mm)		5	5		5
8. Nitrogen supplying pressure (Pa)	Mixing	1.47×10^4	1.47×10^4		1.47×10^4
	Extruding	9.8×10^4	4.9×10^4		1.47×10^4
9. Extrusion rate of polymer solution (m/s)		0.09	0.11		0.09
10. Bore liquid flow rate (m/s)		0.27	0.27		0.27
11. Water bath temperature (°C)		40	40	55	40
12. Take-up speed (m/s)		0.19, 0.32, 0.38	0.19, 0.32, 0.38	0.19, 0.32, 0.38	0.19, 0.32, 0.38

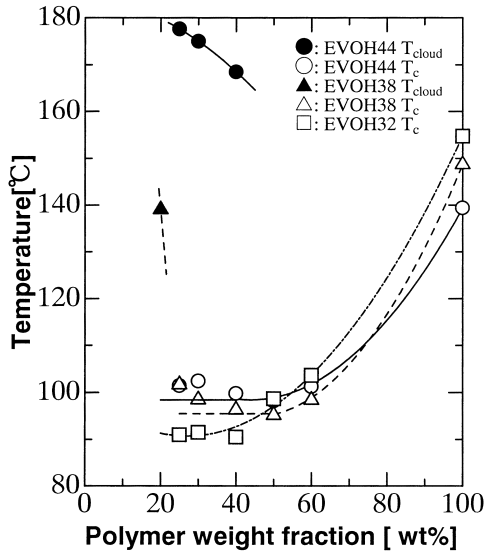

Fig. 1. Phase diagrams for various EVOHs with different ethylene contents. — EVOH44; -- EVOH38; -.-.-.- EVOH32.

shows maximum by Eq. (1):

$$\Lambda = \frac{\lambda_0}{2n_0 \sin\left(\frac{\theta}{2}\right)} \quad (1)$$

Here, n_0 is the refractive index and λ_0 is the wavelength in vacuo (633 nm). The time courses of Λ are shown in Fig. 3 for these three systems. Λ at the same elapse of time increased with the increase of EC. For EVOH44, the binodal temperature is much higher than the crystallization temperature as shown in Fig. 1, which thermodynamically allows the droplets formed by the liquid–liquid (L–L) phase separation to grow for a relatively longer time period compared with EVOH38 and EVOH32 systems, because the binodal line locates below the crystallization line in these two latter systems. Since the binodal point was observed at 20 wt% sample in EVOH38 system, the binodal temperature at 25 wt% sample is closer to the crystallization temperature than in EVOH32 system. Thus, the droplet growing time interval, which is the time interval from the occurrence of

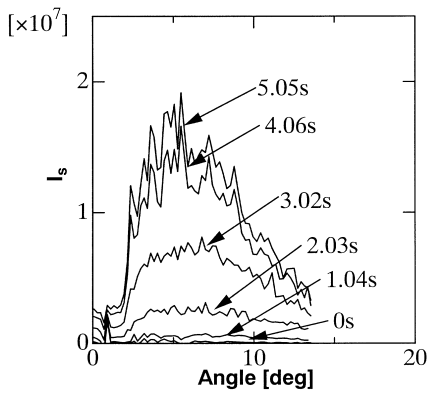

Fig. 2. Light scattering profiles for EVOH38 sample cooled from 160 to 40 °C at the constant rate of 130 °C/min. (polymer concentration: 25 wt%).

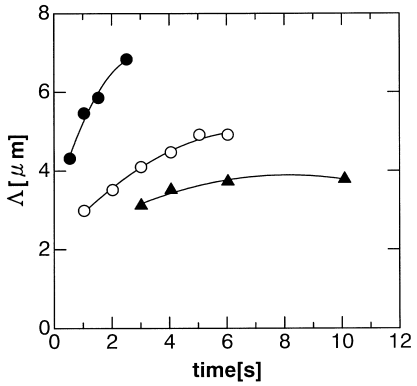

Fig. 3. Time-course of periodic distance Λ in polymer samples at the cooling rate of 130 °C/min. ●: EVOH44; ○: EVOH38; ▲: EVOH32.

the liquid–liquid phase separation to the structure solidification by the crystallization, increases in the order of EVOH32, EVOH38 and EVOH44. This is the reason that Λ increased in this order.

3.3. Structure of hollow fiber membrane

Fig. 4 shows a typical hollow fiber membrane structure prepared from EVOH32 melt blend. The whole cross-sectional structure and its enlarged structure are shown in Fig. 4(a) and (b). Fig. 4(c) and (d) show the cross-sectional structures near the outer and inner surface and Fig. 4(e) and (f) show the outer and inner surface structures. The outer diameter, the inner diameter, and the membrane thickness can be obtained by a measurement from Fig. 4(a) and (b), and the values of this membrane are 698, 419, and 140 μm, respectively. As shown in Fig. 4(c), the skin layer at the outer surface was formed due to the increase of the polymer concentration brought about by the diluent evaporation [12]. The pore size just below the skin layer shown in Fig. 4(c) is larger than that near the inner surface shown in Fig. 4(d), indicating that the membrane structure is asymmetric. In the TIPS process, the higher polymer concentration brings about the smaller pore size [6,16]. Therefore, the smaller pores usually form at the outer surface due to the higher polymer concentration brought about by the diluent evaporation [14]. However, in this case, the polymer solution immersed in the water bath firstly separates into polymer-lean phase and polymer-rich phase by TIPS because heat transfer is generally about two order faster than mass transfer in liquids [21]. Then, water penetrates into the membrane from the outer surface due to the good compatibility between glycerol and water. Subsequently, the water in the membrane mainly exists in the droplets of polymer-lean phase, because the polymer-lean phase almost consists of glycerol. Therefore, the larger pores were formed near the outer surface. On the other hand, as the diluents used in the usual TIPS process are not compatible with water, water cannot penetrate into the membrane. Comparison between Fig. 4(e) and (f) indicates that the porosity at

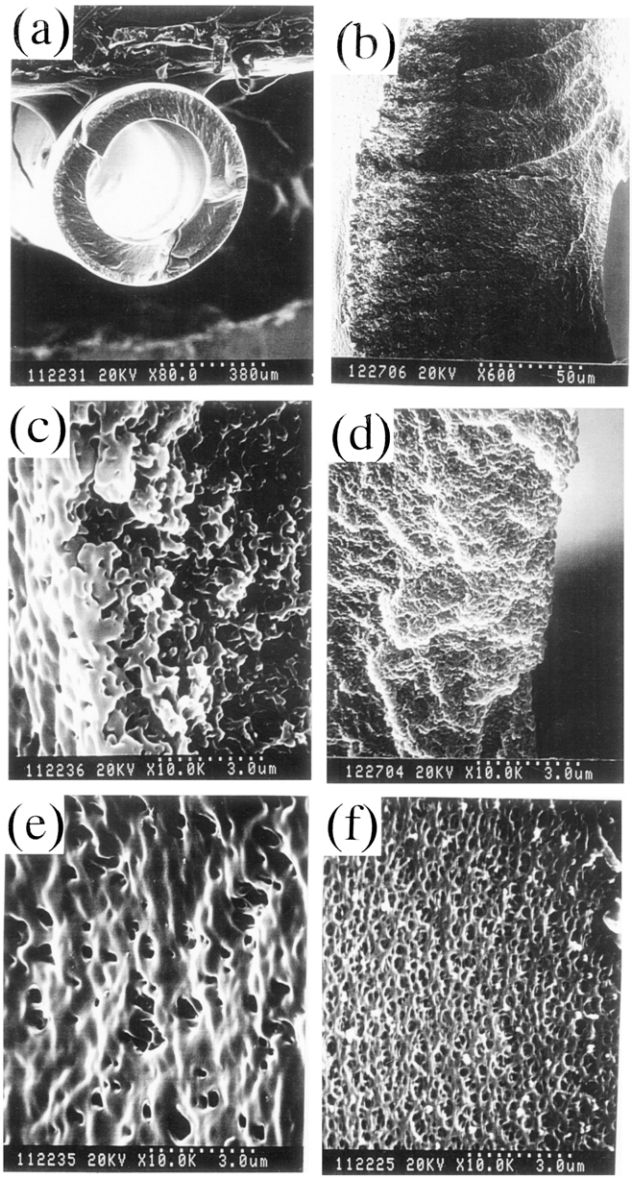

Fig. 4. SEM images of the hollow fiber membranes prepared from EVOH32 solution. (Take-up speed: 0.38 m/s; water bath temperature: 40 °C.) (a) Whole cross-section; (b) enlarged cross-section; (c) cross-section near the outer surface; (d) cross-section near the inner surface; (e) outer surface; (f) inner surface.

the outer surface is smaller than that at the inner surface. Considering the fact that the diluent evaporates when the extruded polymer solution flows from the spinneret to the water bath, the polymer concentration at the outer surface will be higher than that at the inner surface, which leads to the smaller porosity at the outer surface [14].

3.4. Water permeability

3.4.1. Effect of ethylene content (EC)

Effects of take-up speed and EC on water permeability were investigated for three kinds of membranes prepared from different EVOHs with 44, 38, and 32 mol% of EC. The polymer concentration and the water bath temperature were fixed at 25 wt% and 40 °C, respectively. The obtained water permeability is shown in Fig. 5. The water permeability was slightly influenced by the take-up speed; that is, the permeability increased with an increase in the take-up speed, although it was not clear for EVOH44 due to the extremely low permeability. The pores formed by phase separation were enlarged to the drawing direction during spinning. Therefore, the faster take-up speed leads to the larger pores and results in an increase in the water permeability. It is also shown in Fig. 5 that the permeabilities were quite different from each other, and the permeability increased in the order of EVOH44, EVOH38, and EVOH32.

The membrane structures near the inner surface in three systems are shown in Fig. 6(a)–(c). The pore size increased in the order of EVOH32, EVOH38, and EVOH44. This tendency agreed with the light scattering results described in Fig. 3. Fig. 6(d)–(f) show the membrane structures near the outer surface in three systems. In the case of EVOH44, liquid–liquid phase separation continued for the longer time, which changed the porous structure from the initial interconnected structure to the island-like structure and led to the larger pore. Thus, the pores were isolated each other and the pore connectivity was worse. This is the reason for the lowest permeability shown in Fig. 5 although the pore size was larger. On the other hand, the inter-connected structure was obtained in the case of EVOH32 because the liquid–liquid phase separation was fixed in the early stage by the crystallization. Thus, in this case, the pore connectivity determined the water permeability rather than the pore size.

In the case of EVOH44 membrane, no appreciable difference in pore size was found between the structure near the outer surface shown in Fig. 6(f) and the structure near the inner surface shown in Fig. 6(c). It means that the effect of water penetration is very small. This is because water hardly penetrated into this membrane, which can be seen in the result of the extreme low water permeability shown in Fig. 5.

3.4.2. Effect of water bath temperature

The effect of water bath temperature on water permeability is shown in Fig. 7. The water permeability was

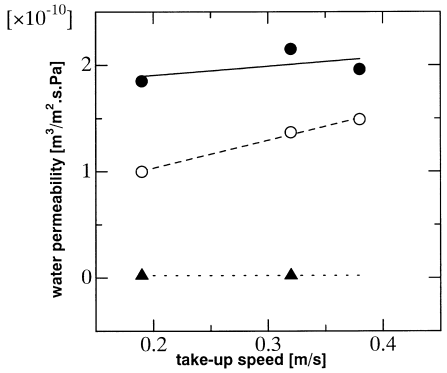

Fig. 5. Effect of EC in EVOH on water permeability. (Water bath temperature: 40 °C) ●: EVOH32; ○: EVOH38; ▲: EVOH44.

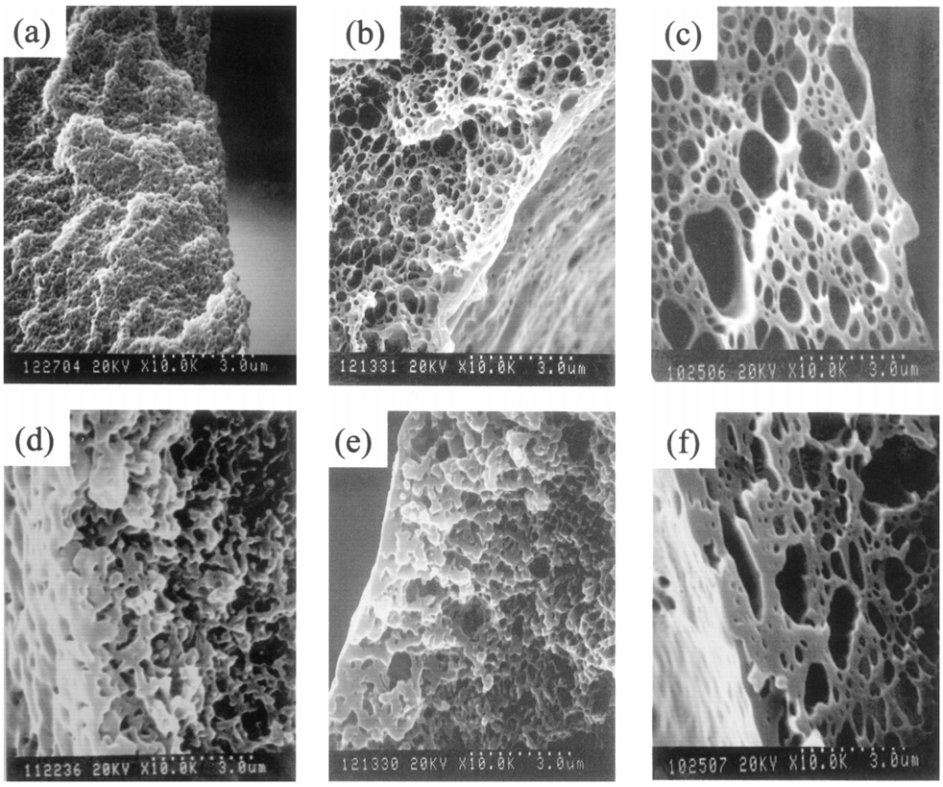

Fig. 6. SEM images of membrane structures. (Take-up speed: 0.38 m/s; water bath temperature: 40 °C.) (a), (b), and (c): near the inner surface; (d), (e), and (f): near the outer surface. (a), (d): EVOH32; (b), (e): EVOH38; (c), (f): EVOH44.

higher in the case of 55 °C bath temperature than that in the case of 40 °C bath temperature at the same take-up speed condition. The dependency of the take-up speed was more pronounced in the case of 55 °C bath temperature. When the bath temperature is high, the polymer membrane is not likely to be solidified by the crystallization because the crystallization rate is slow. This makes the hollow fiber easy to be elongated by the take-up winder. Thus, the effect of the take-up speed on the permeability is more sensitive at the high temperature condition.

Fig. 8 shows cross-sectional membrane structures near the outer surface and outer surface structures obtained in two conditions of 55 and 40 °C bath temperatures. As described above, the higher temperature suppresses the membrane solidificaition. Thus, a large amount of water can penetrate into the polymer solution, which leads to the larger pores near the outer surface, as shown in Fig. 8(a). Furthermore, the droplet formed by the liquid-liquid phase separation can sufficiently grow in the higher temperature condition and larger pores were formed at the outer surface, as shown in Fig. 8(b). This larger pore formation brought about the higher permeability.

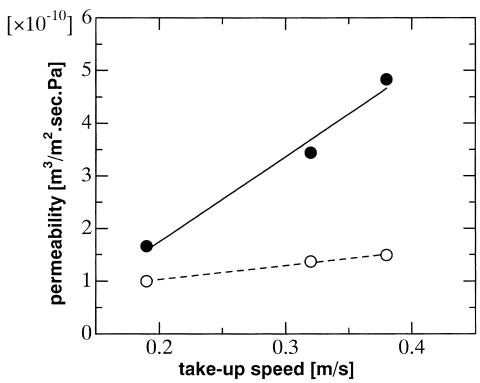

Fig. 7. Effect of water bath temperature on water permeability of EVOH38 membrane. ●: water bath temperature = 55 °C; ○: water bath temperature = 40 °C.

3.5. Solute rejection

The solute rejection coefficient R is defined as

$$R = 1 - C_f/C_0 \quad (2)$$

where C_0 and C_f are solute concentrations in the feed and the filtrate, respectively. Effect of the ethylene content EC on the rejection coefficient is shown in Fig. 9(a). Both the membranes showed high rejection coefficients for polystyrene particle with 20 nm diameter. This means that the EVOH membranes prepared by this process have ultrafiltration property. Fig. 9(b) shows the effect of the water bath temperature. At the bath temperature of 55 °C, the pore size at the outer surface was larger and the solute rejection became lower. However, the particle with 100 nm diameter was still almost rejected by this membrane.

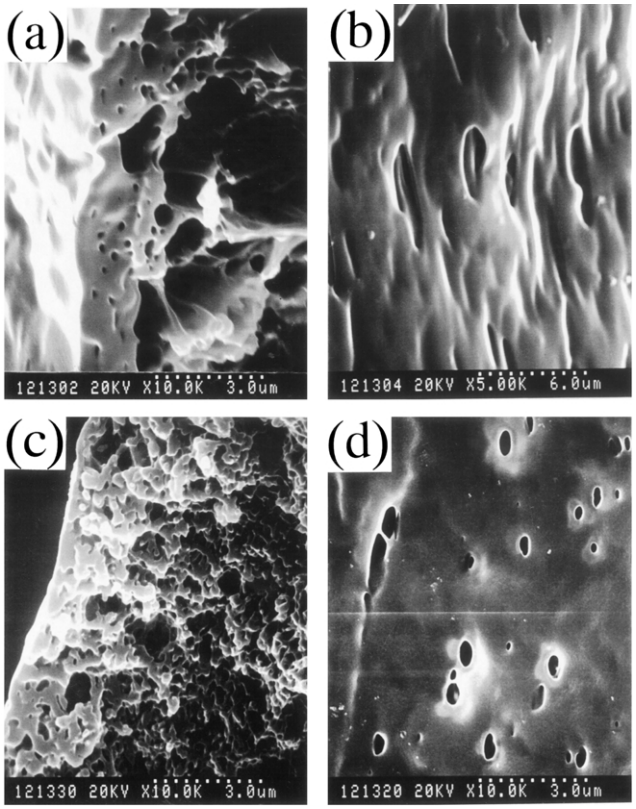

Fig. 8. Cross-sectional structures near the outer surfaces and outer surface structure of EVOH38 membranes. (Take-up speed: 0.38 m/s) water bath temperature: 55 °C: (a) cross-section, (b) outer surface; water bath temperature: 40 °C: (c) cross-section, (d) outer surface.

4. Conclusion

Microporous hollow fiber membranes were prepared from EVOH/glycerol solutions via TIPS. For all membranes, asymmetric structures with the larger pores near the outer surface were obtained. This is due to the enhanced pore growth by the water penetration into the hollow fiber membrane because of the good compatibility between diluent (glycerol) and water.

The phase diagrams were determined for these three systems of EVOH32, 38 and 44. As ethylene content EC increased, the binodal line shifted to the higher temperature region. For EVOH44 and EVOH38 systems, the phase separation occurred by the liquid–liquid phase separation in the lower polymer concentration region. On the contrary, the binodal line shifted below the crystallization line for EVOH32 system.

The phase separation kinetics were investigated by the light scattering measurements. The larger structure was obtained in the system with the higher EC due to the longer coarsening time brought about by the higher binodal temperature.

The higher water permeability was obtained for the membranes prepared from the solution of EVOHs with lower EC. This was achieved by the better pore connectivity

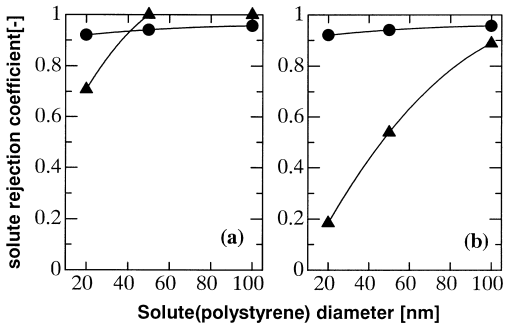

Fig. 9. Solute rejection results. (Take-up speed: 0.38 m/s) (a) Effect of ethylene content EC. (Water bath temperature: 40 °C) ●: EVOH38; ▲: EVOH32. (b) Effect of water bath temperature for EVOH38. ●: 40 °C; ▲: 55 °C.

rather than by the larger pore size. The water permeability could also be improved by increasing the water bath temperature. The prepared hollow fiber membrane had the high solute rejection property. The particle with 20 nm diameter was almost rejected, which indicated that the membrane can be utilized as the ultrafiltration membrane.

References

[1] Mulder M. Basic Principles of Membrane Technology, 2nd ed. Dordrecht, The Netherlands: Kluwer Academic Publishers; 1996. Chapter 8.
[2] Starov VM, Smart J, Lloyd DR. J Membr Sci 1992;103:257–70.
[3] Lloyd DR, Kinzer KE, Tseng HS. J Membr Sci 1990;52:239–61.
[4] Lloyd DR, Kim SS, Kinzer KE. J Membr Sci 1991;64:1–11.
[5] Kim SS, Lloyd DR. J Membr Sci 1991;64:13–28.
[6] Matsuyama H, Iwatani T, Kitamaru Y, Teramoto M, Sugo N. J Appl Polym Sci 2001;79:2449–55.
[7] Matsuyama H, Iwatani T, Kitamaru Y, Teramoto M, Sugo N. J Appl Polym Sci 2001;79:2456–63.
[8] Matsuyama H, Kobayashi K, Maki T, Teramoto M, Tsuruta H. J Appl Polym Sci 2001;82:2583–9.
[9] Liu B, Du QG, Yang YL. J Membr Sci 2000;180:81–92.
[10] Burghardt WR. Macromolecules 1989;22:2482–6.
[11] Matsuyama H, Yuasa M, Kitamura Y, Teramoto M, Lloyd DR. J Membr Sci 2000;179:91–100.
[12] Kim JJ, Hwang JR, Kim UY, Kim SS. J Membr Sci 1995;108:25–36.
[13] Sun H, Rhee KB, Kitano T, Mah SI. J Appl Poly Sci 2000;75: 1235–42.
[14] Matsuyama H, Okafuji H, Maki T, Teramoto M, Kubota N. J Membr Sci in 2003; in press.
[15] Doi Y, Matsuda K, Kono M. Japan Patent 1-38505; 1989.
[16] Shang MX, Matsuyama H, Maki T, Teramoto M, Lloyd DR. J Appl Poly Sci 2003;87:853–60.
[17] Shang MX, Matsuyama H, Maki T, Teramoto M, Lloyd DR. J Poly Sci: Part B: Poly Phys 2003;41:194–201.
[18] Fu SS, Matsuyama H, Maki T, Teramoto M. Sep Purif Technol 2003; in press.
[19] Iwata H, Saito K, Furusaki S, Sugo T, Okamoto J. Adsorption characteristics of immobilized metal affinity membrane. Biotechnol Prog 1991;7:412–8.
[20] Nunes SP, Inoue T. J Membr Sci 1996;111:93–103.
[21] Matsuyama H, Takida Y, Maki T, Teramoto M. Polymer 2001;43: 5243–8.